

文章编号 1004-924X(2011)09-2284-09

# 利用三光束激光干涉仪评估纳米平台的移动性能

王世华\*, 陈秀玲, 徐 淦

(国家计量中心 新加坡科技研究局, 新加坡 118221)

**摘要:** 纳米位移传感器多集成在纳米平台的平行移动柔性机构中, 通过闭环控制回路来实现纳米级的平台移动精度, 本文介绍了利用具有亚纳米分辨率的三光束单频激光干涉仪校正纳米级电容式线性移动平台位移的工作, 阐述了校正测试系统的布局以及线位移和角度位移的校正测试原理。通过实验成功地对移动线位移  $320\ \mu\text{m}$  的纳米平台进行了校正, 实验数据表明, 该平台的偏摆最大角位移为  $3.5''$ 。另外, 对该校正系统进行了测量不确定度分析, 在覆盖因子  $k=2$  时, 它的扩展不确定度为  $(1.8+1.23\times 10^{-2}L)\text{nm}$ , 测试长度  $L$  的单位是  $\mu\text{m}$ , 由此显示该系统可有效评价纳米平台的移动性能。

**关键词:** 电容式纳米平台; 纳米位移传感器; 激光干涉仪

**中图分类号:** TH703; TH744.3 **文献标识码:** A **doi:** 10.3788/OPE.20111909.2284

## Evaluation of nano-stage movement by using triple-beam laser interferometer

WANG Shi-hua\*, TAN Siew-leng, XU Gan

(National Metrology Centre, Agency for Science, Technology and Research, Singapore 118221)

\* Corresponding author, E-mail: wang\_shihua@nmc.a-star.edu.sg

**Abstract:** Nanosensors are generally integrated into flexure translation stages to form a closed-loop feedback to control the movement of the stage accurately in a nano-scale order. To evaluate the displacement of nano-stages, a calibration system based on a single frequency triple-beam laser homodyne interferometer with a sub-nanometre resolution was developed to calibrate the precision of the linear nano-stage with a capacitive feedback sensor. The triple-beam configuration and its linear and angular measuring principles were described to reflect how the linear and angular displacements (yaw & pitch) of the stage could be determined accurately. The experimental results demonstrate that the system is capable of calibrating the nano-stage with a linear displacement up to  $320\ \mu\text{m}$  and an angular deviation up to  $3.5''$ . The error sources of the proposed calibration system were also highlighted in the measurement uncertainty analysis, and it shows that the expanded uncertainty of measurement with a coverage factor  $k=2$  is estimated as  $(1.8+1.23\times 10^{-2}L)\text{nm}$ , where  $L$  is the displacement in  $\mu\text{m}$ . The results

demonstrate that the proposed system can evaluate the movement performance of nano-stages efficiently.

**Key words:** capacitive nano-stage; nanosensor; laser interferometer

## 1 Introduction

Nanosensors—such as capacitive sensors, LVDTs (Linear Variable Differential Transformer), strain gauge sensors and optical encoders (e. g. Moiré and Holographic scales), are commonly used in nanoscale measuring systems. These sensors are usually used on moving stages, together with PZT actuators in a closed loop, to monitor and control the motion of the stages and to minimize errors caused by nonlinearity associated with the performance of the stage. Therefore, the calibration of the stage motion rather than the individual feedback sensor is more practical and meaningful. The calibration of such devices with nanometre uncertainties, and even sub-nanometre uncertainties, has been demonstrated by using X-ray interferometry<sup>[1-3]</sup> and optical interferometry with Fabry-Perot method<sup>[4-6]</sup>. However, these methods are usually very expensive, complex in structures so that they are not suitable for in-situ calibration. From the practical point of view, heterodyne and homodyne laser interferometers<sup>[7-10]</sup> with enhanced interpolation resolutions are preferred as they are relatively simple and very stable under well controlled ambient conditions.

It is worth noting that the relevant systems described above for nano-stage calibration are applied to measure linear displacement only. Those systems may not be ideal to ensure the nanoscale measurement accuracy if the stage cannot provide sufficiently straight motion due to the yaw and pitch angular deviations of the flexure hinge fixture in the stage. Therefore, a system capable of measuring both linear and angular displacements is required for the nano-stage cali-

bration.

In this paper, a nano-stage calibration system allowing both linear and angular displacements to be measured simultaneously is described. The capability of the system is demonstrated through the calibration of a nano-stage with a capacitive feedback sensor.

## 2 Method

Fig. 1 shows the schematic diagram of the triple-beam laser interferometer system based on Michelson interferometry. A collimated laser beam is reflected by mirror 1 ( $M_1$ ) and mirror 2 ( $M_2$ ). Through the polarizer (P) and quarter-wave plate (Q), the laser beam is directed to the three beam splitters ( $B_1$ ,  $B_2$  and  $B_3$ ). The laser beam reflected by the three beam splitters and reflectors ( $R_1$ ,  $R_2$  and  $R_3$ ) is split into three beams, named the trip-beam. This triple-beam as object beam is directed to the plane mirror (M) which is attached to the moving target. The reflected triple-beam superimposes with those reference beams reflected from the fixed reference mirror (R) and the corresponding interference signals are received by the three photodiodes ( $PD_1$ ,  $PD_2$  and  $PD_3$ ), respectively.

The resulting interference (the square of amplitude factor) can be written as:<sup>[11]</sup>

$$y^2 = 4A^2 \cos^2(\pi n F \delta / \lambda), \quad (1)$$

Where  $y$  and  $A$  represent a certain magnitude of the electrical fields and the maximum amplitude of the electrical wave respectively;  $\lambda$  is the wavelength of the light beam;  $\delta$  is the Optical Path Difference (OPD) between object beam and reference beam;  $n$  is the refractive index of the air in the light path;  $F$  is the interferometer factor determined by the interpolation ratio of the electronics.

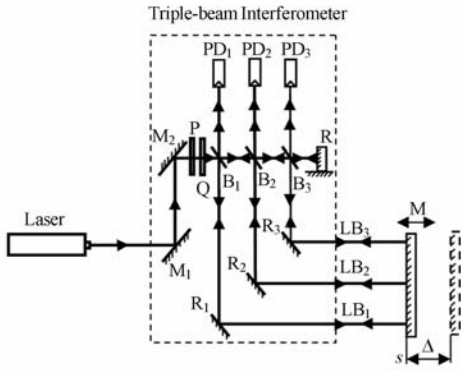


Fig. 1 Schematic diagram of triple-beam laser interferometer

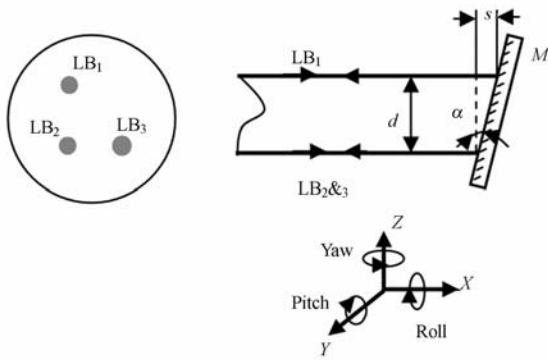


Fig. 2 Detailed view of three laser beams on measuring target

The displacement  $\Delta$  can be determined as:

$$\Delta = m \frac{\lambda}{2n \cdot F}, \quad (2)$$

where  $m$  is the number of the interference fringes introduced by the movement of the moving target. By using advanced signal-process electronic technology, the interferometer is capable of offering extremely high optical path resolution. From Eq. (2), in the case of a 0.1 nm resolution, the factor  $F$  can be as high as 3,164.

As shown in Fig. 2, the angular displacement ( $\alpha$ ) introduced by the tilt of the measuring mirror ( $M$ ) can be determined as:

$$\alpha = \arctan(s/d), \quad (3)$$

where  $s$  is the differential displacement between any two laser beams directed to the measuring target;  $d$  is the separation of the two laser beams. The yaw and pitch angular deviations can therefore be calculated in terms of the differenti-

al displacement when one laser beam is arranged at the crossing position of the  $Y$  and  $Z$  axes and another two laser beams are aligned along the  $Y$  and  $Z$  axes respectively.

### 3 Nano-stage calibration system

Fig. 3 shows the block diagram of the nano-stage calibration system. The system consists of a triple-beam laser interferometer and a PZT translation nano-stage with a capacitive feedback sensor. The laser interferometer and the stage are both controlled by the computer through electronics and control units. Each displacement step introduced by the stage is measured by the laser interferometer synchronously and the data collected are further processed by the computer.

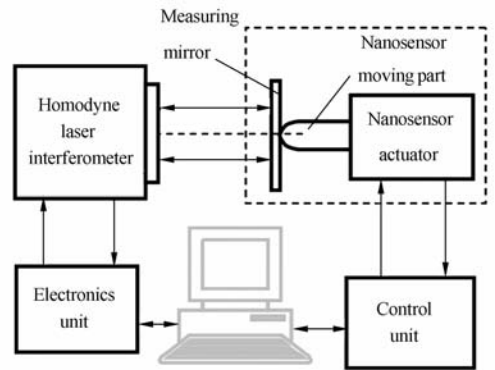


Fig. 3 Block diagram of proposed system for calibration of nano-stage movement

Fig. 4 shows a photo of the calibration system. In the system, a triple-beam laser interferometer (manufactured by SIOS Meßtechnik GmbH, Germany) is able to measure a displacement in a resolution of 0.1 nm. The frequency stabilized He-Ne laser source calibrated by the primary iodine stabilised He-Ne laser is coupled into the interferometer by a single mode fibre. This arrangement makes the triple-beam laser interferometer compact and least sensitive to the thermal influence from the laser head and related electronics. In Fig. 5, the triple-beam laser which enables the system to carry out measurements of angular displacements including yaw

and pitch deviations of the moving stage can be seen on the plane mirror attached to the stage.

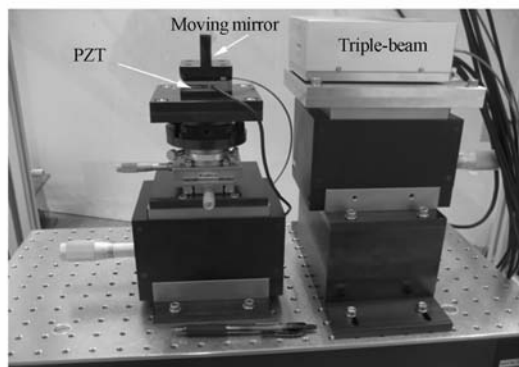


Fig. 4 Photo of experimental set up



Fig. 5 Photo of three laser spots on measuring mirror

It is noted that those optics of the laser interferometer and the nano-stage attachment are rigidly fixed to a super-invar plate and the plane mirror of the interferometer is fixed to the top moving part of the nano-stage. In addition, there are tilt and three-axis translation stages to support the nano-stage as well as the plane mirror so as to adjust the stage moving direction in parallel to the axis of the laser beams.

## 4 Results and discussion

### 4.1 Measurement stability

To ensure a high performance of the calibration system, the measurement stability is verified. Due to the drifts arising from the mechanical, electrical and optical parts in the system consisting of the laser interferometer, stage, device

under test, *etc.*, the stability deteriorates during the measurement. In our system, while the moving mirror is fixed without any displacement, the reading from the laser interferometer during a period of 600 s is obtained and shown in Fig. 6. The maximum integral effect to the measurement stability is found to be less than 3.5 nm. The present system is mounted on a passive anti-vibration table and housed in a single-layer perspex enclosure. So, the drift is expected to reduce if the system is housed in a better acoustically-designed enclosure.

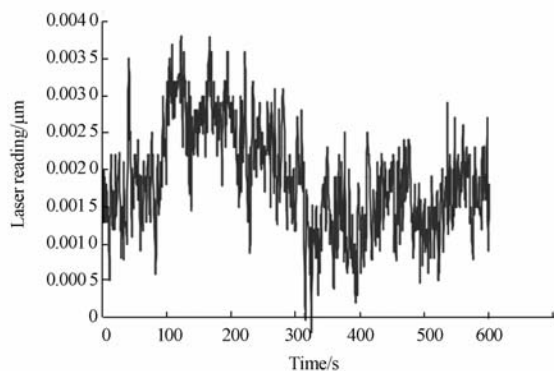


Fig. 6 Drifting records of overall system while nano-stage remains stationary for 10 min

### 4.2 Measurement non-linearity

According to the specifications of the nano-stage furnished with a capacitive feedback sensor, the nano-stage can move up to 320  $\mu\text{m}$  with a resolution of 1 nm. The performance of the nano-stage movement is evaluated over a few ranges.

Firstly, the performance of the nano-stage movement in a short range less than 40 nm is evaluated. When the voltage applies to the PZT actuator integrated with the nano-stage is increased at a 5 mV interval, the top plate is moved step by step with a nominal displacement of 5 nm as shown in Fig. 7. However, it can be seen that the moving step is non-uniform. By using a best fitting, the relation of the stage displacement ( $S$ ) to the applied voltage ( $V$ ) is obtained as  $S = 1.25 V$ . Fig. 8 clearly shows the nonlinearity of the stage within a moving range of 40 nm, which is denoted by the discrete meas-

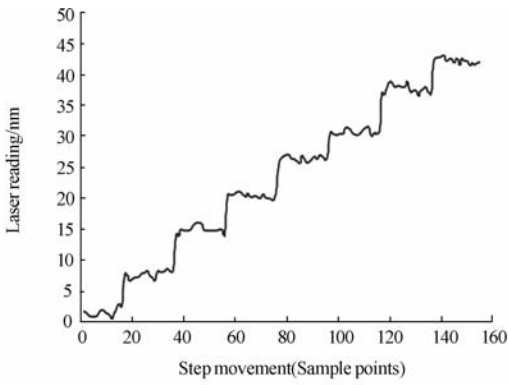


Fig. 7 A typical plot of the laser readings while the nano-stage moves at a nominal step of 5 nm with an interval voltage of 5 mV applied to the PZT actuator in the nano-stage

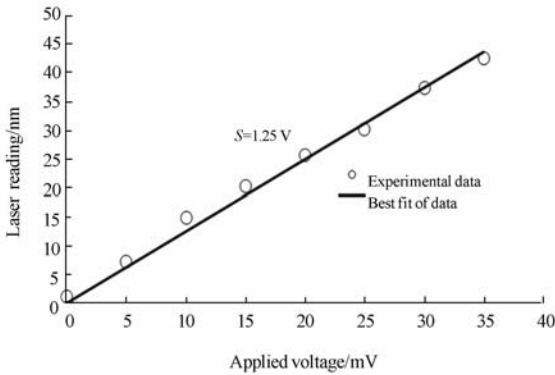


Fig. 8 Relationship between displacement and applied voltage within a range of 40 nm

uring points away from the fitted line. The nonlinearity within the range of 40 nm is about 6%. The nonlinearity in percentage is defined as the maximum displacement deviation over the movement range. Similarly, when the applied voltage is increased at a 10 mV interval, the top plate is moved step by step with a nominal displacement of 10 nm as shown in Fig. 9. As shown in Fig. 10, the movement nonlinearity is decreased to be 3% when the movement range is increased to 100 nm. The decrease in nonlinearity with the increase in a movement range may indicate that the displacement deviation of the nano-stage movement less than 100 nm is not related to the increase of voltage applied to the PZT. Since the maximum displacement deviation up to 3 nm in the range of 40 nm and 100 nm is close to the

value of the system stability (3.5 nm) as discussed in section 4.1, this may imply that the nonlinearity performance of the nano-stage movement less than 100 nm is mainly limited by the stability of the system.

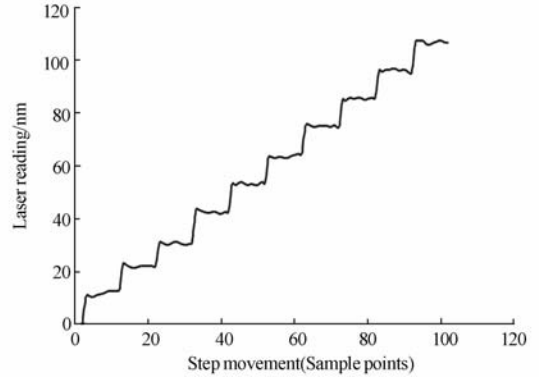


Fig. 9 A typical plot of the laser readings while the nano-stage moves at a nominal step of 10 nm with an interval voltage of 10 mV applied to the PZT actuator in the nano-stage.

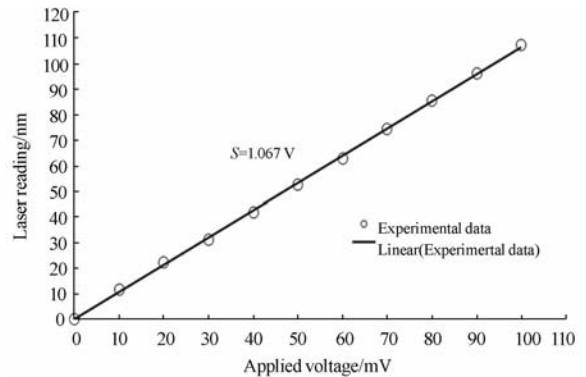


Fig. 10 Relationship between displacement and applied voltage within a range of 100 nm

Secondly, the performance of the nano-stage movement in a long range up to 320  $\mu\text{m}$  is also evaluated. As shown in Fig. 11 and 12, when the applied voltage is increased at a 10 V interval, the top plate is moved step by step with a nominal displacement of 10  $\mu\text{m}$ . The relation of the stage displacement versus the applied voltage is obtained as  $S = 997.54 \text{ V}$ . As the maximum deviation from the fitted line is less than 0.5  $\mu\text{m}$ , the nonlinearity less than 0.2% is favourably achieved.

Lastly, besides the evaluation of the linear

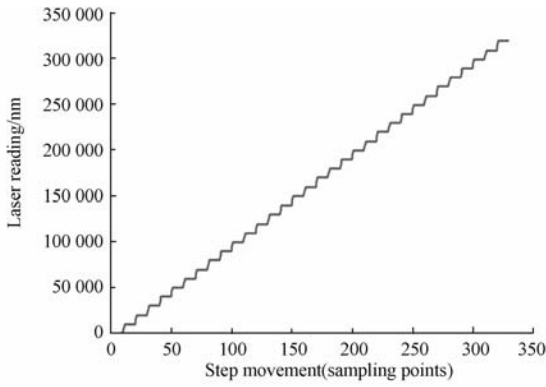
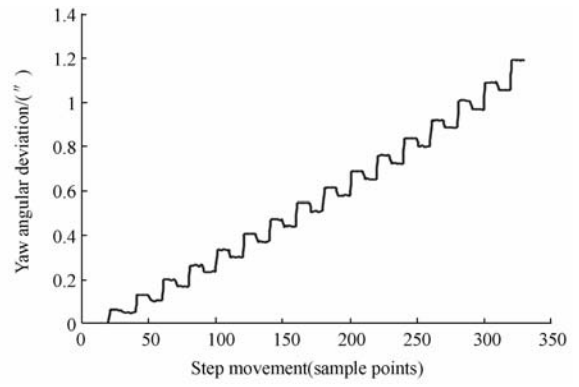


Fig. 11 A typical plot of laser reading while the nano-stage moves at a nominal step of 10  $\mu\text{m}$  with an interval voltage of 10 V applied to PZT actuator in nano-stage.



(b)

Fig. 13 Measurement results of pitch (a) & yaw (b) angular deviations in a range of 320  $\mu\text{m}$

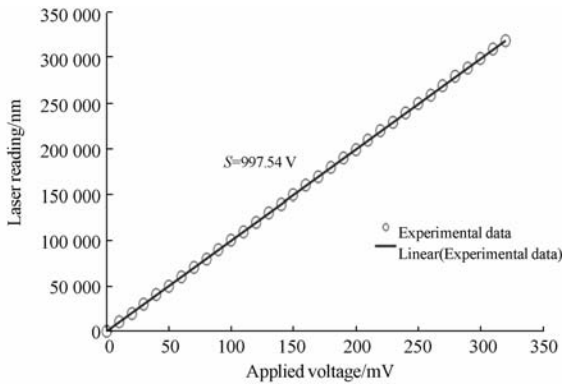
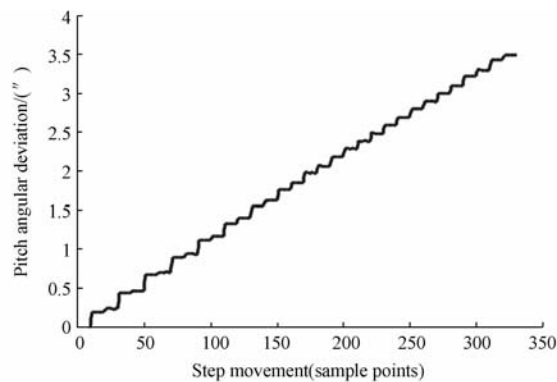


Fig. 12 Relationship between displacement and applied voltage within a range of 320  $\mu\text{m}$

displacement of the nano-stage as shown in Fig. 13, its pitch angular deviation up to 3.49'' and yaw angular deviation up to 1.18'' are measured using the calibration system. The measured



(a)

angles can be used to evaluate the straightness of the flexure mechanism in the nano-stage and to compensate and correct the nonlinearity of the movement.

## 5 Uncertainty analysis

The uncertainties of the calibration system mainly come from two sources: 1) the laser interferometer and 2) the alignment mechanism. The following is a list of possible uncertainty sources for the system.

### 5.1 Laser wavelength stability

The laser frequency is stabilised within  $2 \times 10^{-9}$ . The uncertainty of the laser wavelength mainly comes from the determination of the refractive index of air. With the real time compensation of the environmental conditions including air temperature, air pressure and relative humidity, it can be controlled within  $0.2 \times 10^{-6}$ .

### 5.2 Wavelength compensation

The compensation unit monitors the environmental conditions (air temperature, air pressure and relative humidity) and provides compensation for the effect of these parameters on the wavelength (in air) of the laser beam during measurements. Using Edlen equation<sup>[12]</sup>, the uncertainty of this compensation is typically less than  $0.5 \times 10^{-6}$ .

### 5.3 Optical nonlinearity

The optical non linearity of the homodyne laser interferometer is typically less than  $0.3 \text{ nm}^{[13-15]}$ .

### 5.4 Instability

The instability of the system is contributed by the mechanical instability and electronics noise. The instability in root mean square of the total noise in the system is found to be  $0.5 \text{ nm}$ . The resulting uncertainty is taken as  $0.5 \text{ nm}$ .

### 5.5 Abbe error

The estimated offset of the measurement axis from the motion axis of the stage is estimated to be  $5 \text{ mm}$ . The maximum resulting Abbe error ( $\delta \tan \varphi$ , where  $\delta$  is the Abbe offset,  $\varphi$  is the angular deviation of the stage) is approximately  $0.5 \text{ nm}$ . (Resolution of the angular measurement is  $0.02''$ ).

### 5.6 Cosine error

The cosine error is caused by the misalignment of the laser beams with respect to the direction of the stage movement. It can be eliminated by orientating the laser beam parallel to the actual axis of movement. In our system, the misalignment angle  $\theta$  can be controlled to be less than  $0.2^\circ$ . The resulting cosine error determined by  $(1 - \cos \theta)$  is therefore less than  $6.1 \times 10^{-6}$ .

### 5.7 Optical thermal drift

The physical sizes and the refractive indices of optics (e. g. , mirror, beam splitter, reflector) used in the interferometer vary during measurement. The optical thermal drift factor is typically  $0.04 \mu\text{m}/^\circ\text{C}$ . In our laboratory, the temperature is controlled at  $(20 \pm 1)^\circ\text{C}$  over 24 h. If one round relative measurement is done in less than 10 min, the corresponding temperature fluctuation is less than  $0.01^\circ\text{C}$ . Therefore, the resulting uncertainty is  $0.4 \text{ nm}$ .

### 5.8 Dead path error

The dead path length ( $D_p$ ) is the difference in air-path length between the measurement and the reference beams of the interferometer when the measurement is initiated. Dead path error occurs when there is a non-zero dead path and

environmental conditions change during a measurement. The resulting error is given by:  $E(D_p) = D_p \times \Delta n$ , where  $\Delta n$  is the change in refractive index over the measurement time.

If  $D_p = 1 \text{ mm}$ ,  $\Delta n = 1 \times 10^{-7}$ , the resulting uncertainty is  $0.1 \text{ nm}$ .

### 5.9 Material thermal expansion

Normally, the flexure stage is made of super-invar with a thermal expansion coefficient of  $0.3 \times 10^{-6}/\text{K}$ . The resulting non-compensated thermal drift is estimated to be  $0.3 \times 10^{-6}$ .

**Tab. 1 Uncertainty budget associated with the measurement of the displacement**

Source of Uncertainty	Standard Uncertainty
1 Laser wavelength stability	$0.2 \times 10^{-6}$
2 Wavelength compensation	$0.5 \times 10^{-6}$
3 Optical nonlinearity	$0.3 \text{ nm}$
4 Instability of the system	$0.5 \text{ nm}$
5 Abbe error	$0.5 \text{ nm}$
6 Cosine error	$6.1 \times 10^{-6}$
7 Optical thermal drift	$0.4 \text{ nm}$
8 Dead path error	$0.1 \text{ nm}$
9 Material thermal expansion	$0.3 \times 10^{-6}$
Combined Uncertainty	$0.9 \text{ nm} + 6.13 \times 10^{-6} L$
Expanded Uncertainty	$(1.8 + 1.23 \times 10^{-2} L) \text{ nm}$
$U_L (k=2)$	$L$ is the displacement in microns

Table 1 shows the uncertainty budget of the above evaluation. The combined uncertainty is given by the root sum squared of all the uncertainty components, including the absolute value and the relative value which is length dependent. The expanded measurement uncertainty ( $U_L$ ) is  $(1.8 + 1.23 \times 10^{-2} L) \text{ nm}$ , where  $L$  is the displacement in  $\mu\text{m}$ , estimated at a level of confidence of approximately 95% with a coverage factor  $k=2$ .

## 6 Concluding remarks

The National Metrology Centre of Singapore has developed a nano-stage calibration system using

a triple-beam laser homodyne interferometer. With the use of the triple-beam in a single laser interferometer, the angular deviations (yaw & pitch) of the stage movement are also measured and can be used to evaluate the straightness of the movement in association with the performance of the flexure hinge fixture of the nano-stage. The results show that the nano-stage linear displacement up to 320  $\mu\text{m}$  can achieve a non-linearity less than 0.2% and an angular deviation less than 3.5" due to the effects of pitch and yaw. When measurements are taken over a period of 10 min with the nano-stage operating in

static mode, the expanded measurement uncertainty at 95% confidence level is estimated to be  $(1.8 + 1.23 \times 10^{-2} L)$  nm, where  $L$  is the moving displacement in  $\mu\text{m}$ .

In future work, more efforts will be put to enhance the stability and improve the signal to noise ratio of the system. It is also our intention to take part in international comparison to establish measurement equivalent of the system with others. In addition, as the performance of the system is currently evaluated in the static mode, its performance in the dynamic mode will be further explored.

## References:

- [1] BOWEN D K, CHETWYND D G, SCHWARZENBERGER D R. Sub-nanometer displacement calibration using X-ray interferometer Design [J]. *Meas. Sci. Technol.*, 1990,1:107-119.
- [2] YACOOT A, KUETGENS U S, KOENDERS L, *et al.*. A combined scanning tunneling microscope and x-ray interferometer [J]. *Meas. Sci. Technol.*, 2001,12:1660-1665.
- [3] DOWNS M J, NUNN J W. Verification of the sub-nanometric capability of an NPL differential plane mirror interferometer with a capacitance probe[J]. *Meas. Sci. Technol.*, 1998,9:1437-1440.
- [4] HAITJEMA H, SCHELLEKENS P H J, WETZELS. Calibration of displacement sensors up to 300  $\mu\text{m}$  with nanometre accuracy and direct traceability to a primary standard of length[J]. *Metrologia*, 2000,37:25-33.
- [5] LAWALL J R. Fabry-Perot metrology for displacements up to 50 mm[J]. *J. Opt. Soc. Am.*, 2005, 22:2786-2798.
- [6] BRAND U, HERRMANN K. A laser measurement system for the high-precision calibration of displacement transducers[J]. *Meas. Sci. Technol.*, 1996, 7:911-917.
- [7] TOM T B, LEE J Y, KIM J W, *et al.*. Portable calibration system for displacement measuring sensors [J]. *International Journal of Precision and Manufacturing*, 2006,7(2):56-59.
- [8] PICOTO G B. Interferometric calibration of micro-displacement actuators [J]. *Proceeding of SPIE*, 2003,5190:355-360.
- [9] PUPPIN E. Displacement measurements with resolution in the 15 pm range[J]. *Rev. Sci. Instrum.*, 2005,76:105107.
- [10] JÄGER G. Laser-based measurement to nanometer scale accuracy[J]. *SPIE*, 2001,4420:193-202.
- [11] MOLLER K D. *OPTICS* [M]. California: Mill Valley, 1998.
- [12] BIRCH K P, DOWNS M J. An updated Edlen equation for the refractive index of air[J]. *Metrologia*, 1993,30:155-162.
- [13] BÜCHNER H Jr, JÄGER G. A novel plane mirror interferometer without using corner cube reflectors[J]. *Meas. Sci. Technol.*, 2006,17:746-752.
- [14] JÄGER G, MANSKE E, HAUSOTTE T, *et al.*. Application of miniature interferometers to nanomeasuring and nanopositioning devices [C]. *Proceedings of TEDA Conference "Scanning Probe Microscopy, Sensors and Nanostructures"*, Peking, 2004: 24-17.
- [15] DAI G L, POHLENZ F, DANZEBRINK H U, *et al.*. Improving the performance of interferometers in metrological scanning probe microscopes [J]. *Meas. Sci. Technol.*, 2004,15:444-450.

**Authors' biographies:**

**WANG Shihua**, PhD He works as a Senior Metrologist in the Optical Metrology Department of the National Metrology Centre (NMC) of Agency for Science, Technology and Research (A \* STAR). He is currently involved in the length and dimensional calibration

& measurement in both micro- and nano-scale, particular in carrying out nano-scale measurements using a large range metrological atomic force microscope. His main R&D interests are in laser interferometric surface profiler, length and dimensional measurements, light scattering surface roughness measurement, micro(opto)electromechanical systems testing and optics-mechanical design.



**TAN Siew Leng**. She is the Head of the Optical Metrology Department of the National Metrology Centre of A \* STAR (Agency for Science, Technology and Research). Her main responsibility is to oversee the metrology in length & dimension, photometry & radiometry and time & frequency. She holds an Honours in

Physics and a Master's in the Management of Technology, both from the National University of Singapore. She has over 20 years of expertise in the length & dimensional metrology. She represents Singapore in the International Committee for Weights and Measures (CIPM) Consultative Committee for Length. She is the Chair of the Asia Pacific Metrology Programme (APMP) Technical Committee for Length (TCL). Apart from being a technical assessor for the Singapore Laboratory Accreditation Scheme, she is also involved in many Calibration and Measurement Capability (CMC) intra/inter-Regional Metrology Organisation (RMO) reviews and peer assessments for other national metrology institutes.



**Xu Gan**, PhD, He received his MS and PhD degrees in laser physics from University of Manchester in 1981 and 1983 respectively and worked as a senior research scientist, lecturer and associate professor in a number of universities in UK and China between 1984 and 1991

before joining the National Metrology Centre in 1991 where he is currently a principal metrologist. His research interest covers optical metrology including nanometrology, photometry & radiometry as well as photovoltaics.